Supporting information for: Rationally Designed Semi-conducting 2D Surface Confined Metal Organic Network

Vipin Mishra,[†] Showkat H. Mir,[†] Jayant K Singh,[*,‡] and Thiruvancheril G. Gopakumar[*,†]

†*Department of Chemistry, Indian Institute of Technology Kanpur, Kanpur 208016, India*

‡*Department of Chemical Engineering, Indian Institute of Technology Kanpur, Kanpur 208016, India*

E-mail: jayantks@iitk.ac.in; gopan@iitk.ac.in

Phone: +91 5122596141; +91 5122596830. Fax: +91 5122596806

S1: HOMO-LUMO gap of benzene and its carboxyl derivatives

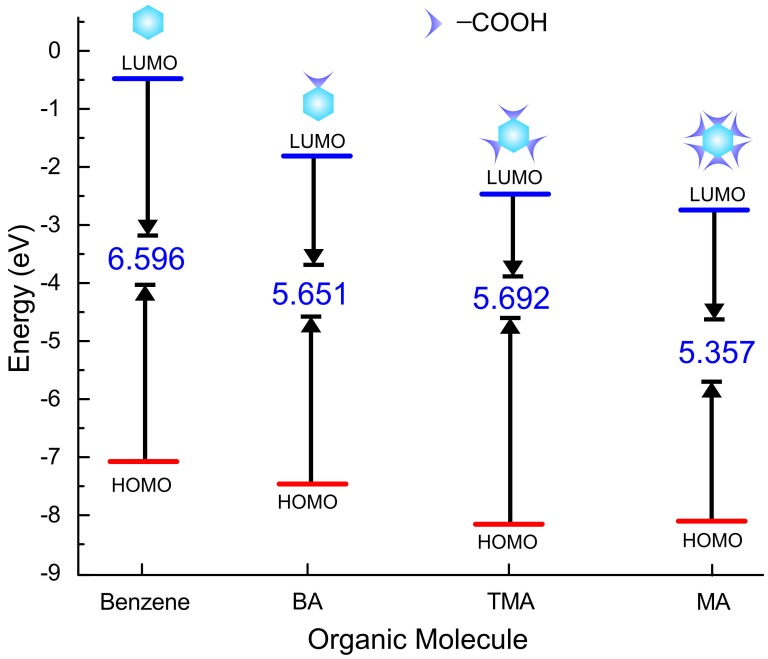

Figure S1: HOMO-LUMO gap of Benzene, Benzoic acid (BA), Trimesic acid (TMA), and Mellitic acid (MA) calculated using B3LYP/6-311g implemented in Gaussian 09.

S2: AFM topographs corresponding to phase images in Figure2

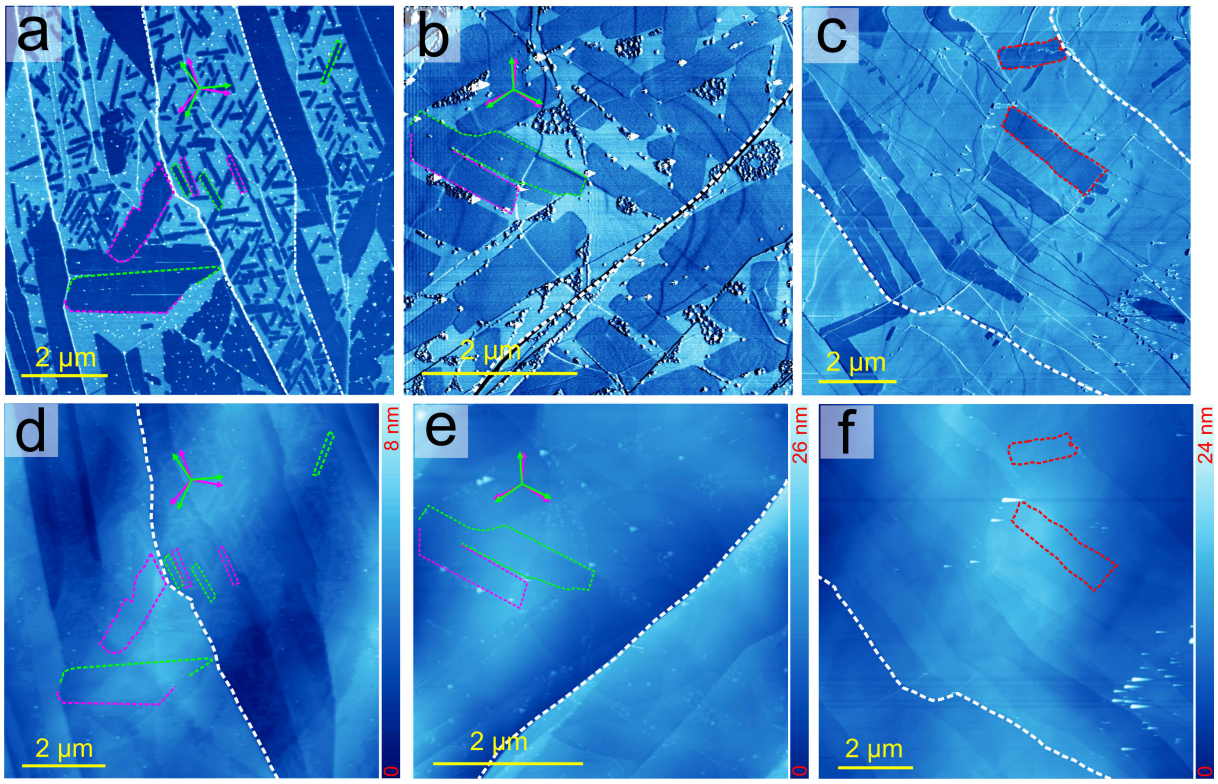

Figure S2: AFM phase image (a, b, and c) and the corresponding AFM topographs (d, e, and f) of MA adlayer (a and d), MA-Pd SMON (b and e), and MA-Zn SMON (c and f). Molecular islands are marked by dashed magenta and green lines. A few graphite terraces are marked using white dashed lines.

S3: Height profile of MA adlayer and SMONs.

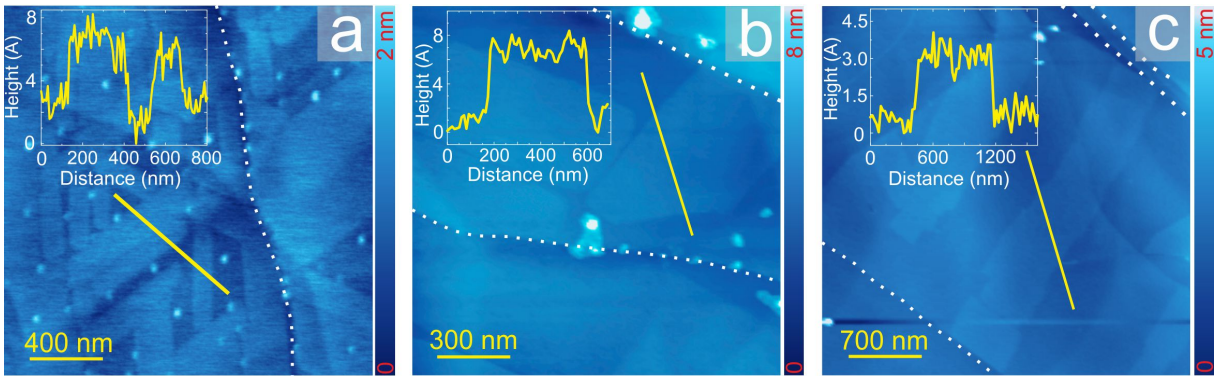

Figure S3: AFM topographs of MA adlayer (a), MA-Pd SMON (b), and MA-Zn SMON (c). In set of each image shows the corresponding height profile along the marked yellow line. A few graphite terraces are marked using white dotted lines.

S4: STM topographs obtained at HOPG-octanoic acid interface

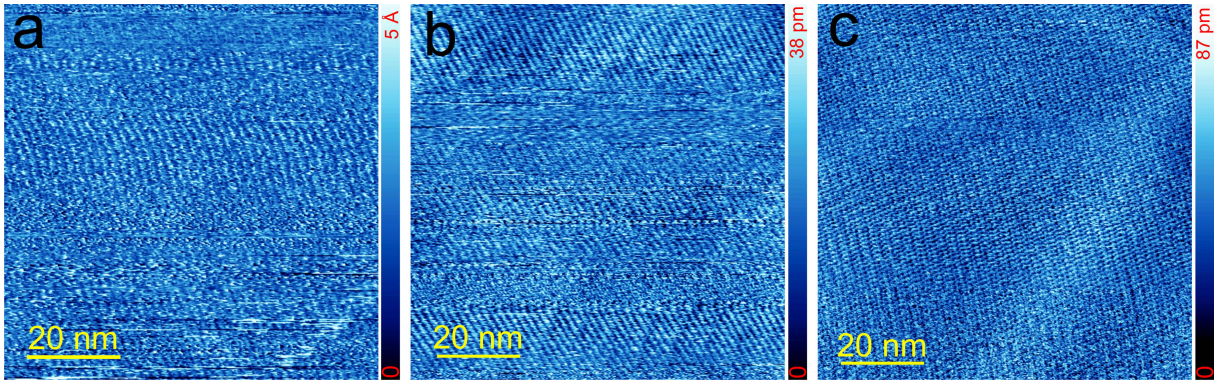

Figure S4: STM topograph of MA adlayer (a), MA-Pd SMON (b), and MA-Zn SMON (c) obtained at HOPG-octanoic acid interface.

S5: Large area STM topographs obtained at solid-air interface

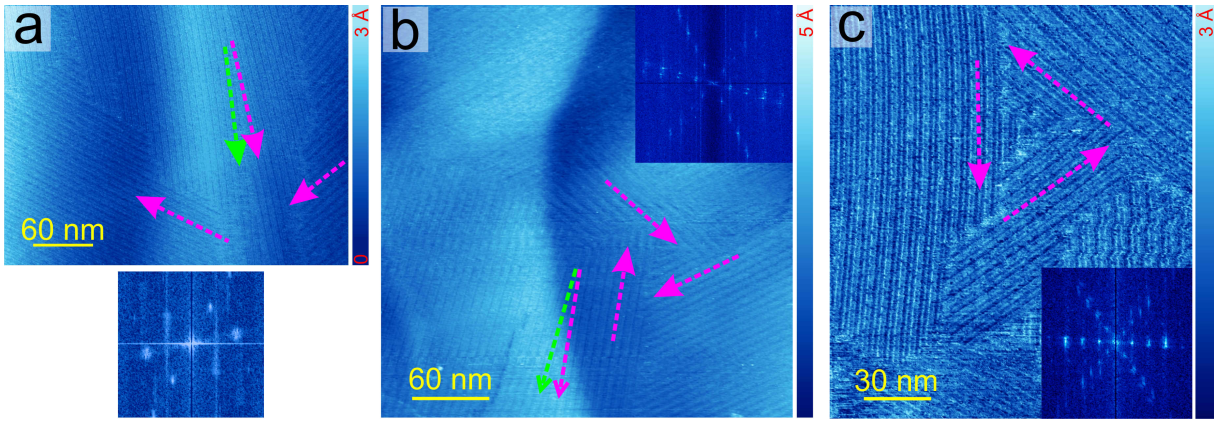

Figure S5: STM topograph of MA adlayer (a), MA-Pd SMON (b), and MA-Zn SMON (c) obtained at solid-air interface. Multiple domains are marked using dashed magenta and green arrows (green arrows show mirror domains). Inset shows 2D FFT of the image where hexagonal bright spots are observed indicating that the domains are following graphite compact lattice directions.

S6: STM topograph obtained at HOPG-air interface

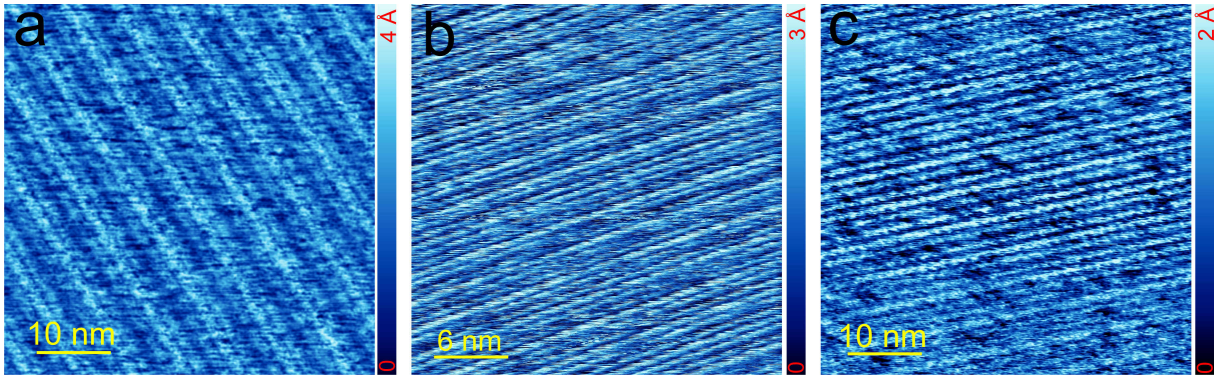

Figure S6: STM topohraphs of MA adlayer (a), MA-Pd SMON (b), and MA-Zn SMON (c) obtained at HOPG-air interface.

S7: Section of chicken-wire pattern of MA

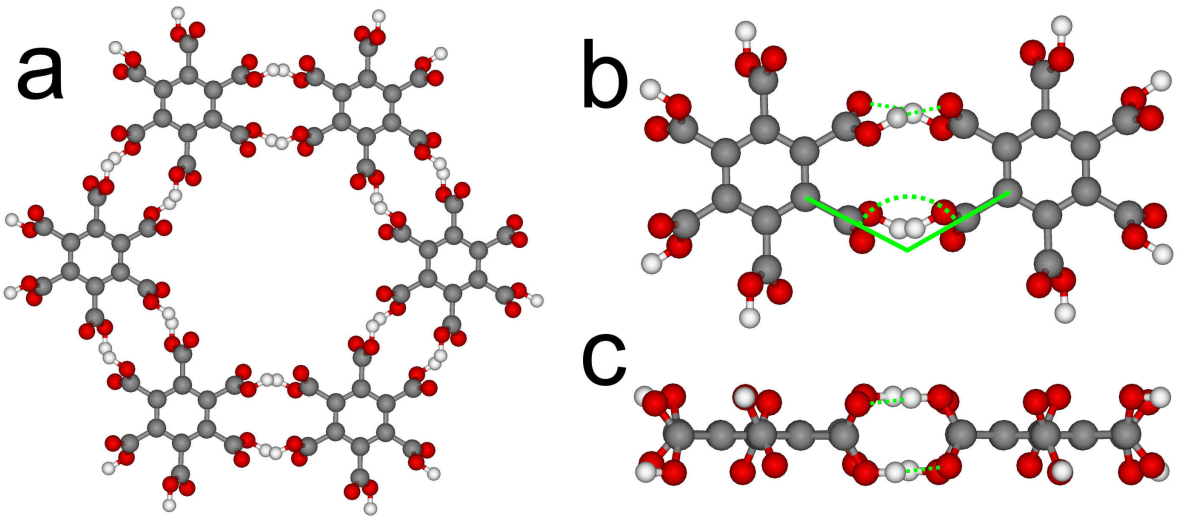

Figure S7: (a) A single hexagonal unit of CW pattern of MA. The top view (b) and side view (c) of dimeric hydrogen bonded two adjacent molecules in CW of MA. Green lines are showing the angle ($\approx 57°$) between two carboxyl group which is forming the hydrogen bonding. The observed angle shows that the hydrogen bonding (O–H$\cdots$O; green dashed lines) groups are nearly linear.

S8: DFT optimized geometry of different patterns of MA

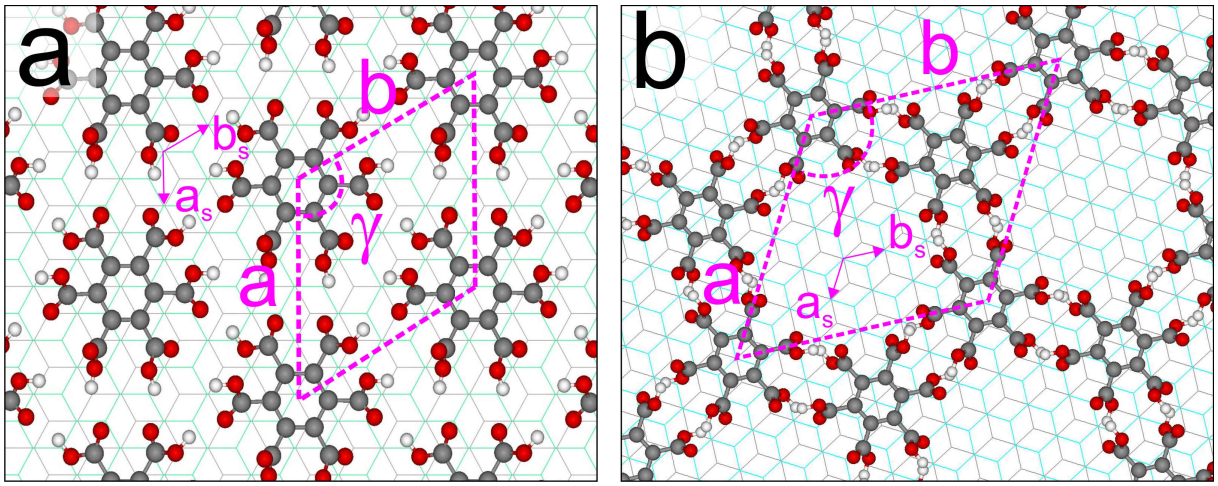

Figure S8: DFT optimized geometry of superflower (SF)(a) and chicken wire (CW)(b) patterns of MA on bilayer graphite. **a**, **b**, and γ are the lattice parameters. $\mathbf{a}_S$, $\mathbf{b}_S$ are the lattice parameters of graphite.

S9: Geometric model for moiré super-lattice

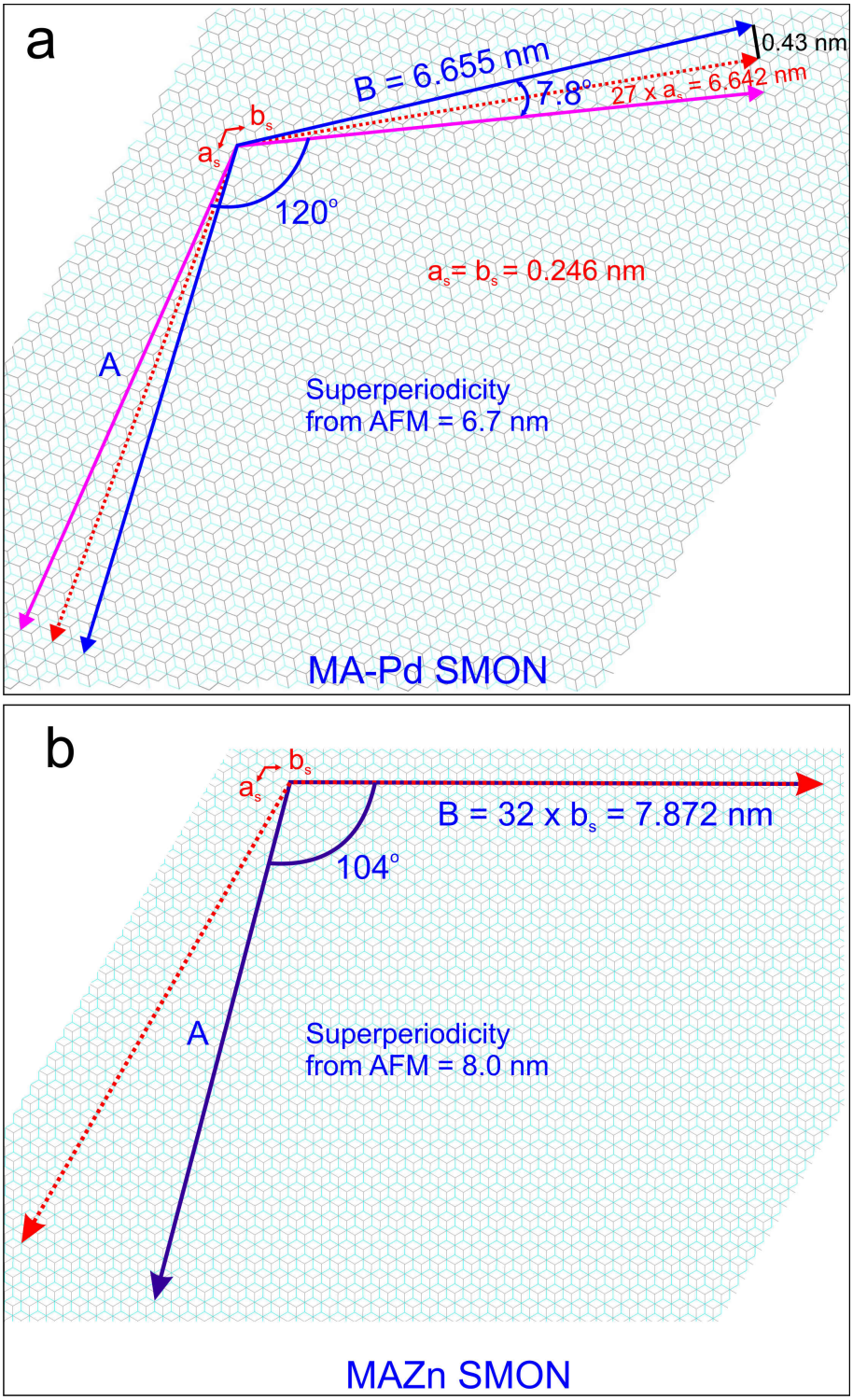

Figure S9: Model justifying the moiré pattern of MA-Pd SMON (a) and MA-Zn SMON (b).

Model justifying the moiré pattern of MA-Pd SMON: Blue and magenta arrows depict the molecular super-lattice with A, B as the super-lattice vectors. Angle between A and B is 120° as obtained from the DFT model. The relative orientation between graphite lattice (red dashed arrow) and molecular lattice is ± 3.9° as obtained from the AFM images. The super-periodicty obtained from the model, A = B = 6.655 nm matches well with that observed in AFM (6.7 nm). a_s and b_s depicts the graphite lattice. Model justifying the moiré pattern of MA-Zn SMON: A, B are the super-lattice vector and angle between A and B is 104° as obtained from STM images. AFM images shows no mirror domains indicating that one of the graphite lattice is aligned with that of MA-Zn SMON. The super-periodicty obtained from the model, A = B = 7.872 nm matches well with that observed in AFM (8.0 nm).

S10: Raw dI/dV data

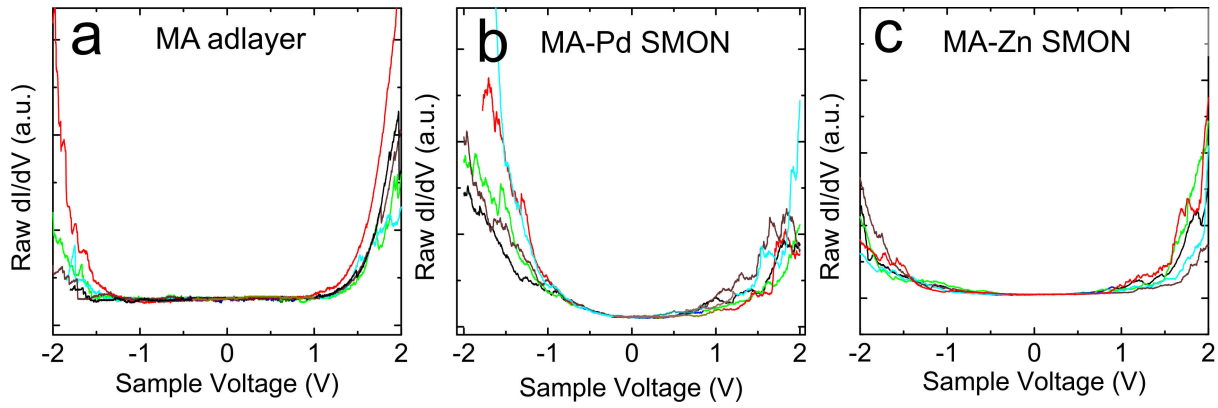

Figure S10: As measured (average) dI/dV on MA adlayer (a), MA-Pd SMON (b), and MA-Zn SMON (c). Different colors indicate different set of averaged independent measurements.

S11: Normalized dI/dV spectra of MA Adlayer

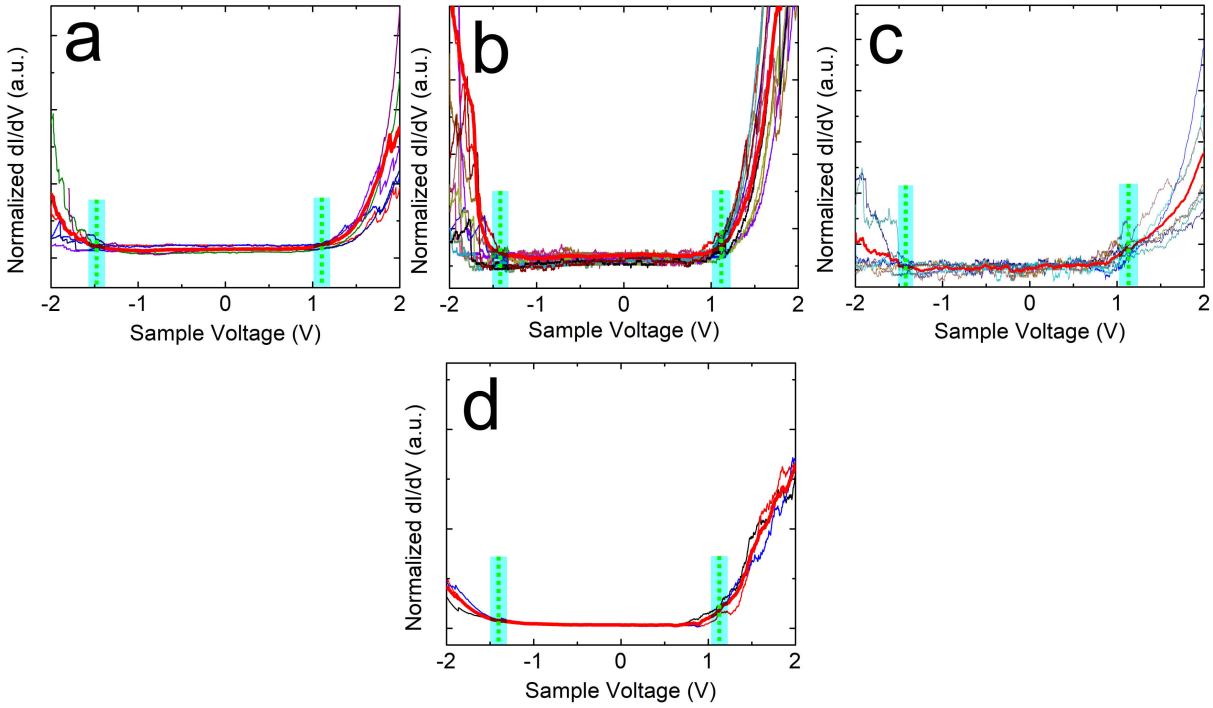

Figure S11: Normalized dI/dV spectra of MA adlayer. a, b, c and d show different set of measurements and the averaged data is shown in red. The averaged data from each set is provided in Figure 4a. The dI/dV measured on HOPG is subtracted from these spectra to obtain the normalized dI/dV. A factored dI/dV of HOPG is subtracted from the raw dI/dV obtained on MA adlayer and SMONs (S12 and S13) as follows,
$dI/dV_{SMON} = dI/dV_{SMON+HOPG} - a \times dI/dV_{HOPG}$.
Factor (a) used for subtraction for MA adlayer is 0.003, MA-Pd SMONs is 0.034 (S12) and for MA-Zn SMON is 0.029 (S13). This procedure is implemented to reduce the influence of graphite density of states (DOS) and is adapted from Mishra et al.[S1]

S12: Normalized dI/dV spectra of MA-Pd SMON

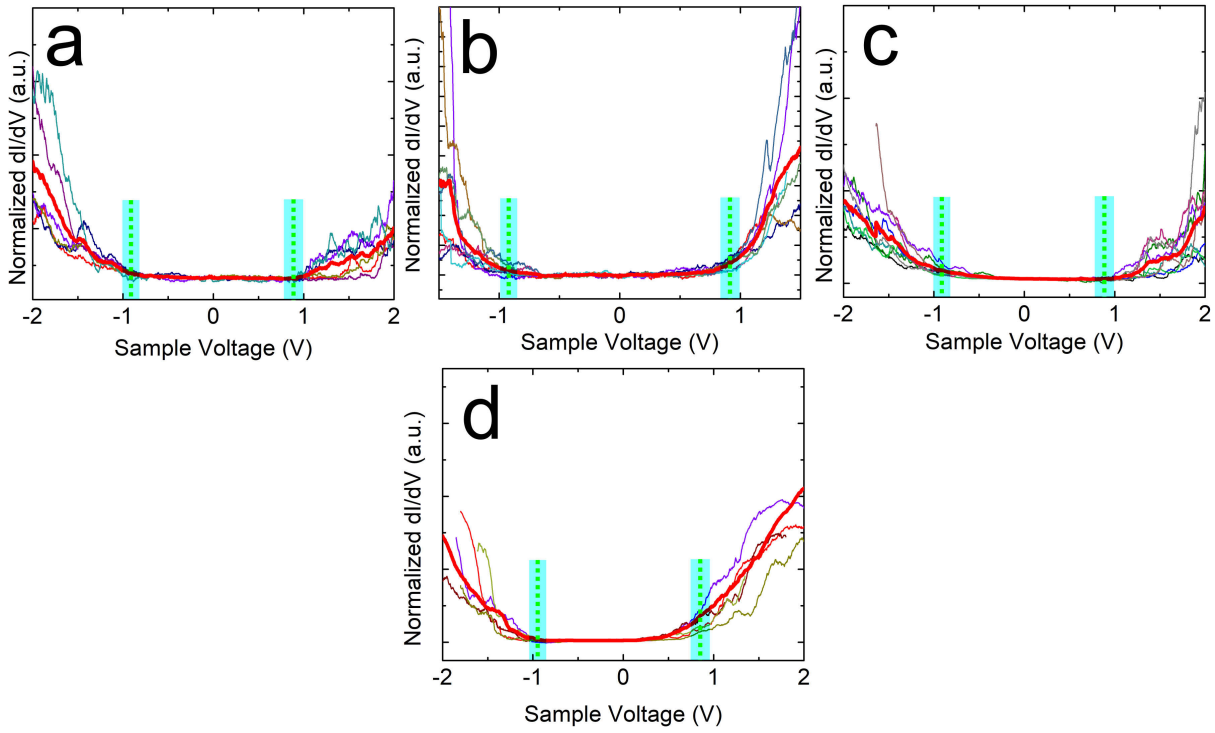

Figure S12: Normalized dI/dV spectra of MA-Pd SMON. a, b, c and d show different set of measurements and the averaged data is shown in red. The averaged data from echa set is provided in Figure 4b.

S13: Normalized dI/dV spectra of MA-Zn SMON

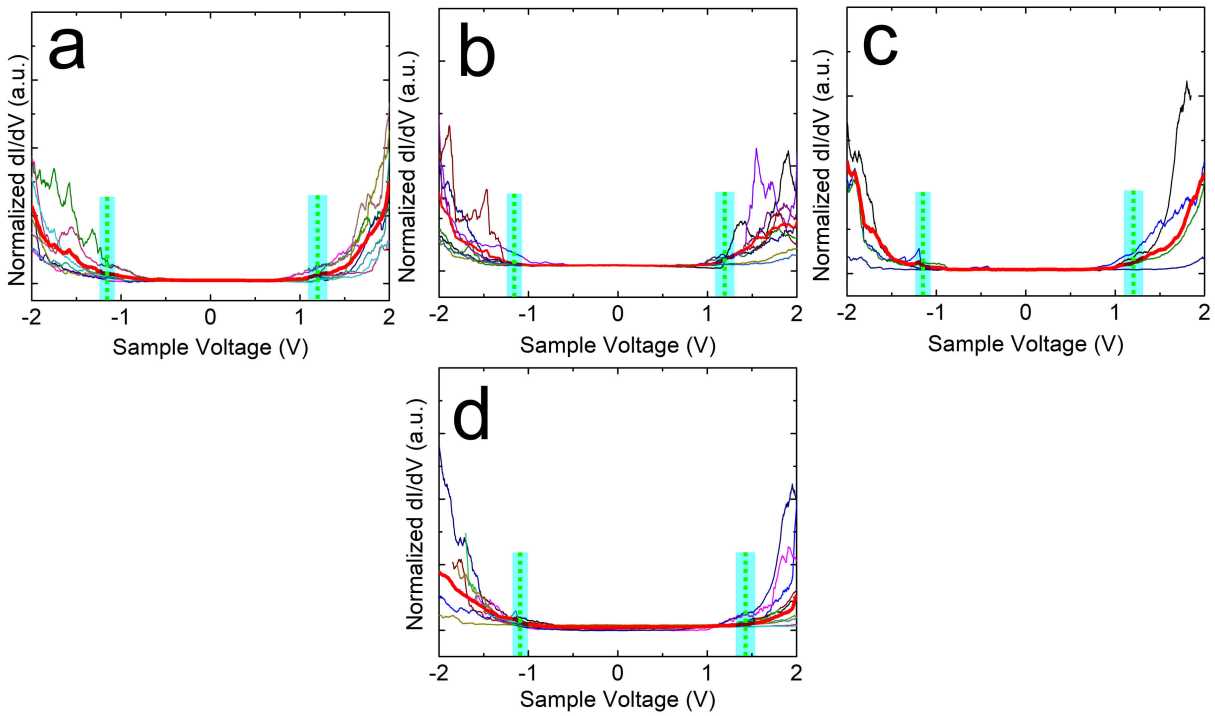

Figure S13: Normalized dI/dV spectra of MA-Zn SMON. a, b, c and d show different set of measurements and the averaged data is shown in red. The averaged data from each set is provided in Figure 4c.

S14: Band structure and DOS of SF-MA adlayer

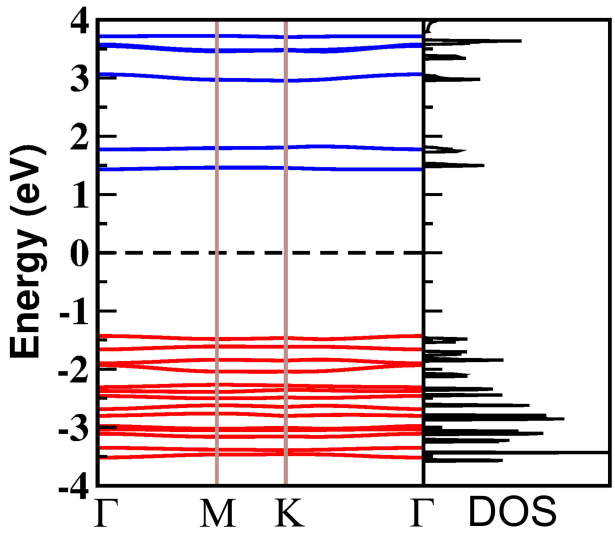

Figure S14: Theoretically calculated band structure and density of state (DOS) of super-flower pattern of MA.

S15: Hubbard corrected band structure and DOS for SMONs

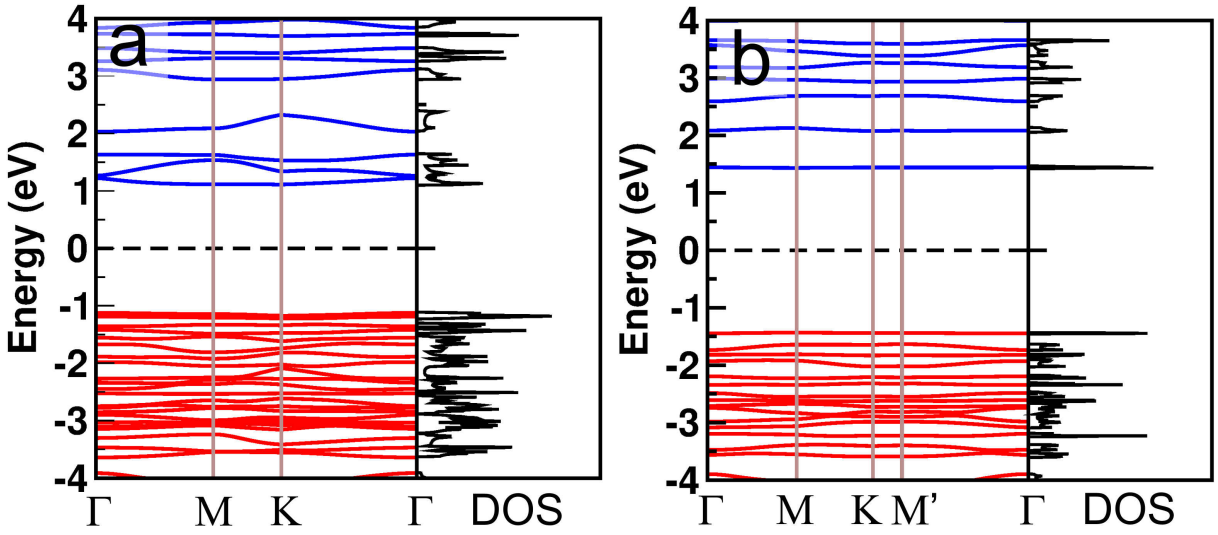

Figure S15: Hubbard corrected (PBE+U) band structure and the corresponding DOS of MA-Pd SMON (a) and MA-Zn SMON (b).

S16: Isosurface plot

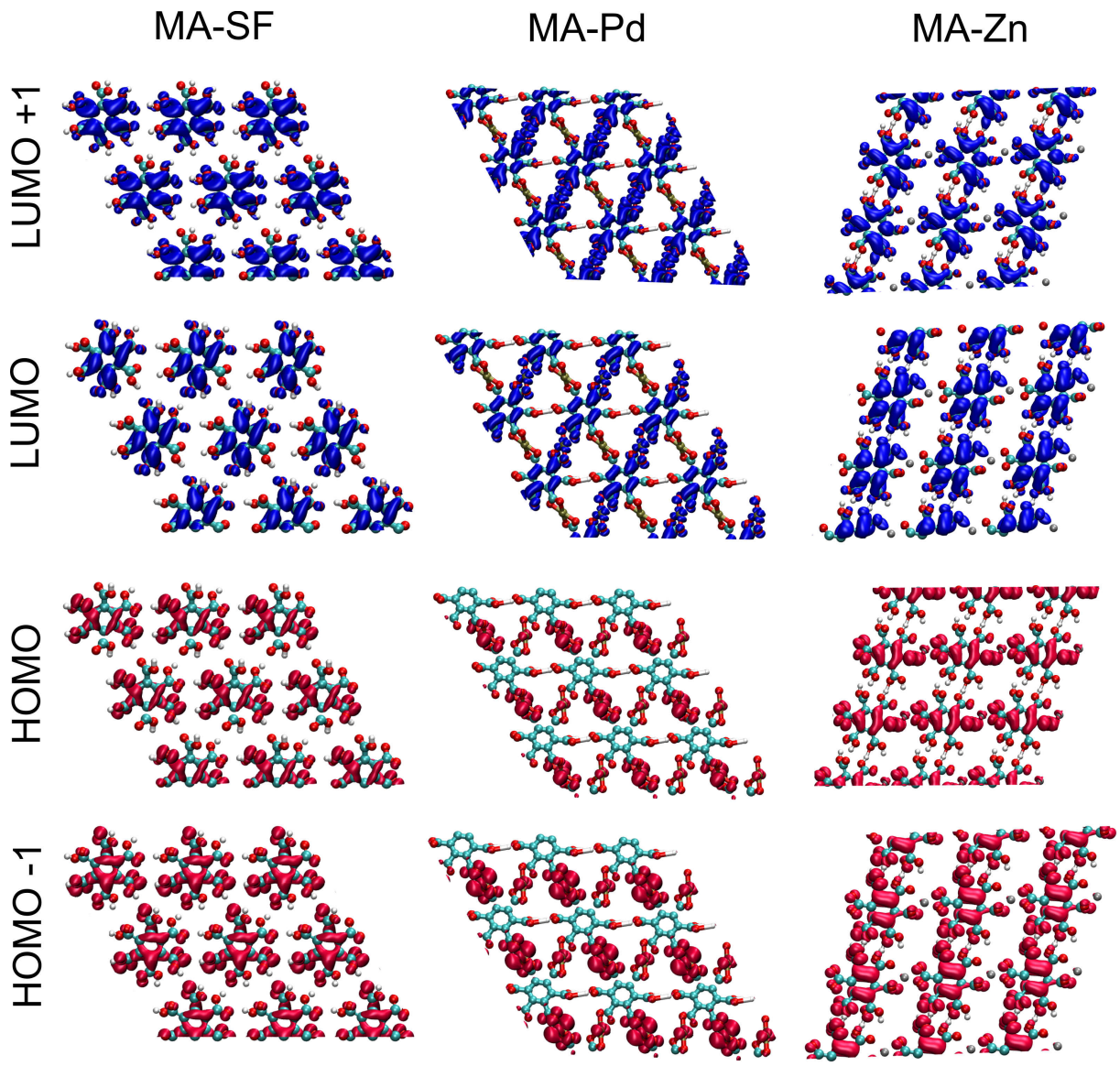

Figure S16: Isosurface plot for the frontier bands (corresponding to HOMO, HOMO-1, LUMO, and LUMO+1) for SF-MA adlayer (a), MA-Pd SMON (b), and MA-Zn SMON (c).

S17: Details of XPS measurements

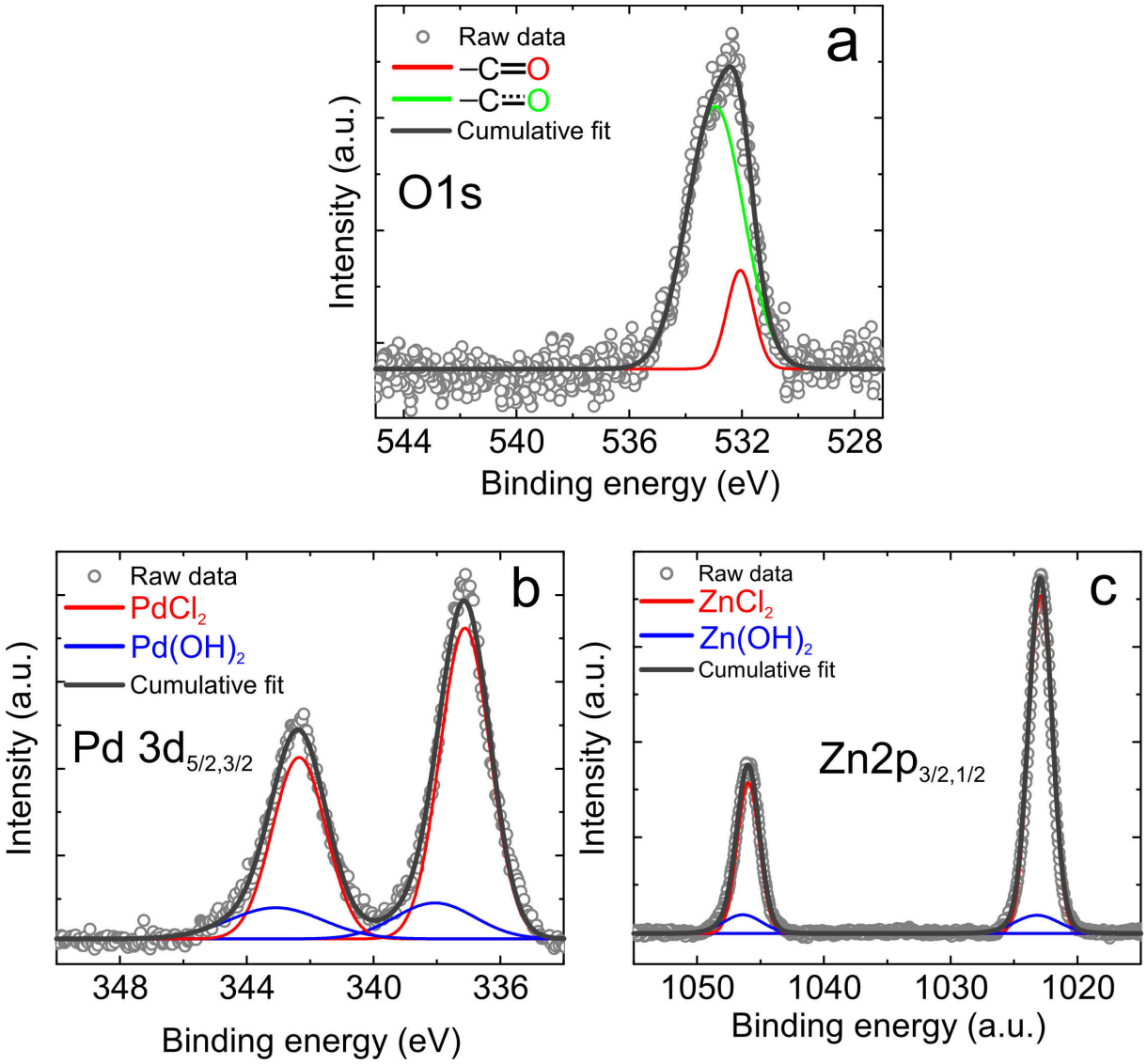

Figure S17: XPS spectra: O1s of MA adlayer (a), Pd3d of $PdCl_2$ (b) and Zn2p of $ZnCl_2$ (c).

The major O1s resonance observed in MA adlayer on HOPG is at 532.9 eV and is corresponding to a hydrogen bonded C=O/C-O group (or partial double bonded C and O).[S2,S3] This indicates that majority of the MA molecules are forming an ordered assembly mediated by dimeric hydrogen bonding of carboxyl groups. This is expected as we have seen large well-ordered crystalline domains of self-assembled MA in AFM images. The minor peak (532.06 eV) corresponding to C=O group suggesting that there are unordered MA on

surface. We have observed small clusters on the surface, which are most likely unordered MA molecules. The major peaks in $PdCl_2$ at 337.11 (342.35) eV correspond to $Pd3d_{5/2}$ ($Pd3d_{3/2}$) resonances. The BE corresponds to Pd(II) oxidation state and is in accordance to the literature for $PdCl_2$.[S4] The shoulder at 338.06 (343.08) eV correspond most likely to the presence of $Pd(OH)_2$ in the salt. The peak value of major resonance observed at 1022.29 (1045.96 eV) in $ZnCl_2$ film correspond to $Zn2p_{3/2}$ ($Zn2p_{1/2}$).[S5] The shoulder at 1023.20 eV corresponds to presence of $Zn(OH)_2$ in the salt.[S6]

Table S1: The Binding energy and FWHM values of O1s, $Pd3d_{5/2}$ ($Pd3d_{3/2}$) and $Zn2p_{3/2}$ ($Zn2p_{1/2}$) resonances in MA adlayer, MA-Pd/Zn SMONs and $PdCl_2$/$ZnCl_2$ films.

Resonances	Binding Energy, eV (FWHM, eV)			
MA O1s	-	532.94 (2.35)	532.06 (1.11)	-
MAPd SMON O1s	535.00 (2.66)	533.15 (1.97)	531.64 (1.79)	-
MAZn SMON O1s	-	532.60 (2.28)	531.90 (1.88)	-
MAPd SMON Pd3d	337.95 (1.12)	338.26 (2.41)	343.20 (1.23)	343.49 (3.00)
PdCl2 Pd3d	337.11 (1.86)	338.06 (2.95)	342.35 (2.00)	343.08 (3.47)
MAZn SMON Zn2p	1022.46 (1.62)	1023.30 (3.77)	1045.50 (1.73)	1046.50 (3.89)
ZnCl2 Zn2p	1022.92 (2.12)	1023.20 (4.12)	1045.96 (2.04)	1046.40 (3.53)

References

(S1) Mishra, V.; Yadav, V. K.; Singh, J. K.; Gopakumar, T. G. Electronic Structure of a Semiconducting Imine-Covalent Organic Framework. *Chem. Asian J.* **2019**, *14*, 4645–4650.

(S2) Lin, N.; Stepanow, S.; Vidal, F.; Barth, J. V.; Kern, K. Manipulating 2D metal-organic networks via ligand control. *Chem. Commun.* **2005**, 1681–1683.

(S3) Sienkiewicz-Gromiuk, J.; Rusinek, I.; Kurach, L.; RzÄ. . . czyńska, Z. Thermal and spectroscopic (IR, XPS) properties of lanthanide(III) benzene-1,3,5-triacetate complexes. *Journal of Thermal Analysis and Calorimetry* **2016**, *126*, 327–342.

(S4) Militello, M. C.; Simko, S. J. Palladium Chloride (PdCl2) by XPS. *Surface Science Spectra* **1994**, *3*, 402–409.

(S5) Seals, R. D.; Alexander, R.; Taylor, L. T.; Dillard, J. G. Core electron binding energy study of group IIb-VIIa compounds. *Inorg. Chem.* **1973**, *12*, 2485–2487.

(S6) Kotsis, K.; Staemmler, V. Ab initio calculations of the O1s XPS spectra of ZnO and Zn oxo compounds. *Phys. Chem. Chem. Phys.* **2006**, *8*, 1490–1498.